Workshop on Visualisation in Environmental Sciences (EnvirVis) (2013)
O. Kolditz, K. Rink and G. Scheuermann (Editors)

Visualizing Saline Intrusion in a Three-Dimensional, Heterogeneous, Coastal Aquifer

M. Walther[1], L. Bilke[2], J.-O. Delfs[2], T. Graf[3], J. Grundmann[4], O. Kolditz[2,5], R. Liedl[1]

[1]Technische Universität Dresden, Institute for Groundwater Management, Dresden, Germany
[2]Helmholtz-Centre for Environmental Research, Department of Environmental Informatics, Leipzig, Germany
[3]Leibniz Universität Hannover, Institute of Fluid Mechanics and Environmental Physics in Civil Engineering, Hannover, Germany
[4]Technische Universität Dresden, Institute of Hydrology and Meteorology, Dresden, Germany
[5]Technische Universität Dresden, Applied Environmental Systems Analysis, Dresden, Germany

Abstract

We visualize remediation scenarios for a coastal aquifer in Oman, where the natural fresh-saltwater interface is negatively affected by groundwater pumping for irrigation. The 3D aquifer is characterized by strong heterogeneities ranging from local to regional scale, which impose visual challenges in the interpretation of large data amounts. This paper addresses the visualization workflow, which helped to ensure correct model setup and successful calibration of a transient model run. The modelling and visualization exercise identified sensitive areas for salinization along the coast and assessed the impact of remediation measures on the groundwater reservoir in space and time. Proper visualization helped to interpret and illustrate the complex results adequately, and to transfer scientific information to stakeholders.

Categories and Subject Descriptors (according to ACM CCS): I.3.3 [Computer Graphics]: Picture/Image Generation—Display algorithms I.3.7 [Computer Graphics]: Three-Dimensional Graphics and Realism—Virtual reality

1. Introduction

In regions with limited surface water availability, groundwater resources are often exploited to satisfy agricultural, domestic or industrial purposes. In coastal and agricultural areas with irrigational demands, pumping activities typically lead to water table drawdown and, as the natural balance of fresh and saline water is disturbed, exacerbate the marine intrusion of saltwater in coastal areas. As saline water cannot be used for irrigation, long-term stability of the fresh-salt water interface is a common goal for water management in (semi-)arid regions.

Numerical models contribute to the development of possible management strategies. However, scientific knowledge is hard to commit to stakeholders and customers because of lack in perception. While a related work presented a visualization of a pore-scale flow field [NBK13], present work focuses on a three-dimensional, heterogeneous watershed. In this case, complex hydrogeological structures consisting of distinct sedimental layers and simulation output must be visualized with care to permit proper interpretation of the 3D data in two-dimensional environments (see also [UKSD12]).

This study extends the work by [WDG*12] by presenting the workflow to visualize results of a transient calibration and a subsequent scenario simulation.

2. Methods and Concepts

Numerical Model. The simultaneous movement of water and salt through an unconfined aquifer is modelled with the finite element code OpenGeoSys for coupled processes in (fractured) porous media (OGS, [KBB*12]). OGS is well established in the field of density-driven flow by a variety of applications (see [BSKL12], [KDS*11], [PA08]). The essential processes (e.g. density-induced convection) are reproduced in standard benchmarks (see [WDG*12], [KGSW12]). Oberbeck-Boussinesq approximation of level 1 accounts for density effects. Even in presence of strong heterogeneities, the water table is flexible in the simulations by employing an approach by [SD87].

DOI: 10.2312/PE.EnvirVis.EnvirVis13.077-081

Study area. The domain is three-dimensional and heterogeneous with an areal coverage of ca. $20 \cdot 30\,\mathrm{km}^2$ and a maximum depth of 450 m in the middle of the model area ("Ma'awil trough"). Boundary conditions (BC) of the model are inflow from the mountains, spatially distributed pumping abstraction, and known sea level and salinity. Hydraulic conductivity, mean annual subsurface inflow from mountainous recharge regions, as well as initial pumping rates are estimated by calibrating the steady-state of 1974 and transient flow until 2005. In order to evaluate the remediation potential of the aquifer, a "best-case" scenario simulation was carried out with the assumption, that all pumping activity was ceased after year 2005. Scenario simulation time was 500 years. Over the period 1974-2005, simulated groundwater levels matched well with measurements near the coast and abstraction area; saline intrusion agrees well with the literature (see [MAF12]).

Visualization Tools. Modelling results are visualized using ParaView (PV, [Hen07]), a data-analysis and visualization application based on the Visualization Toolkit (VTK, [SML06]). VTK employs a filter pipeline model that enables the user to combine a wide variety of visualization algorithms including contouring, glyphing, thresholding, slicing or streamlining. PV offers a client-server architecture to handle large datasets. The server processes the data and generates the visualization on a powerful computer cluster. Results of today's increasingly detailed or regional to larger scale setups often are tremendous data sets, which exceed bandwidth limitations to transfer output data from simulation clusters to local personal computers. Since the computational burden grows according to the detail in modelling and visualization, more and more visualization tools must run directly on the cluster and only transmit pre-rendered, lower sized data packages. Then, only the resulting images are sent to the user client. Data sets of simulation output are $\approx 150\,\mathrm{MB}$ per time step resulting in a total of $\approx 75\,\mathrm{GB}$ for the long-term simulation. Processed and transmitted visualization data from the server are $< 2\,\mathrm{MB}$ per figure.

Remediation potential. To visualize the capability of the system to return to a near-natural state, we define the remediation potential Φ of the upper aquifer from salinity half-life after pump stop in the scenario simulation as

$$\Phi = 1 - c_{\mathrm{rel}} \cdot \frac{\lambda}{\lambda_{\max}} \tag{1}$$

with c_{rel} is relative concentration of salinity 10 m below groundwater level in 2005, λ is half-life of c_{rel}, and $\lambda_{\max}$ is maximum of λ. The qualitative value Φ had to be multiplied with c_{rel} to avoid overestimations for cells with initially already low salinity.

3. Results and Discussion

Water levels and salt loads. Figure 1 shows the groundwater flow field in 2005, which is affected by saline intrusion and abstraction (pumping rates reach highest values). The visualization confirms the expected underground flow regime in the highly heterogeneous domain: high velocities near pumping abstraction and in "Ma'awil" trough in middle of domain (due to highly permeable porous media); variations in fluid density induce vertical convection at the coast; the velocity vector's colouring shows that the freshsaltwater interface reached the location of major abstraction areas. First, the data source was superelevated 10 times in z-direction to increase perceptibility of the flat domain. Then, the visualization was achieved through the combination of two pipelines: i) Isolines of the groundwater surface were generated; ii) velocity vectors are created with size representing the magnitude of velocity and the colour showing relative mass fraction (i.e. salinity).

Saline intrusion pattern. Figure 2 illustrates saline intrusion along the coast 10 m below groundwater level. The isosurface was extracted and coloured according to relative mass fraction. The outline is affected by the local hydrogeology, and spatially distributed pumping activities, which cause a complex flow field (Figure 1). Mean length, temporal trend, and the pattern in saltwater intrusion are similar to published data (2-4 km in 1975 to 5-7 km in 2005). Uncertainties are due to a number of reasons. For instance, structure and parameters of the hydrogeology, as well as abstraction rates of groundwater pumps are not exactly known. Local and short-term recharge events in wadi channels, are not included in the simulation, but might influence short-term groundwater levels and salinity. To obtain a sense of the impact of intensive agriculture to such a coastal area, we notice that intrusion length reduced until 2105, when water abstraction was stopped in 2005 in scenario simulations.

Groundwater flow paths. Two stream tracers, one near the coast and the other one in the southern upstream area, reveal the origin and paths of abstracted groundwater. In combination with relative mass fraction and groundwater levels, the stream tracers lead to the following interpretation: as expected, the initial state 1974 (2a) shows little abstraction near the coast. Upstream recharge plumes, originating in the southern mountainous areas, still reach the sea. As fresh water discharges into the sea, the interface between freshwater and intruding seawater is still retained near the coast. In 2005 (2b), all recharge plumes are completely captured by pumping activities. High abstraction rates lead to immense drawdown and accordingly excessive saltwater intrusion of up to 3 km. The pumping field in the middle of the domain limits water availability further downstream and, thus, might augment saline intrusion near "ADG-23". After 100 years (2c), water from the mountainous recharge areas partly reach the sea again and slowly refills the aquifer storage. Yet, groundwater levels and salinity did not returned to their former values in the 1970s. In order to obtain an equal distribution of the stream tracer's point sources, the following procedure was used: the domain was cut vertically and again 10 m be-

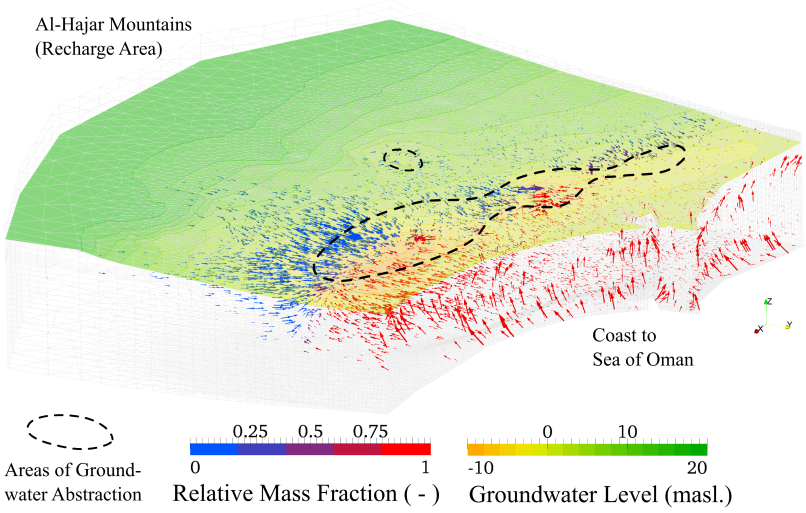

Figure 1: *Groundwater model domain, final state of transient simulation (year 2005); groundwater levels, scaled velocity vectors with relative mass fraction; dashed lines symbolize major areas of groundwater abstraction.*

low groundwater level. Then, equally spaced points were extracted, to provide starting points for the stream tracers. The resulting flow velocities along the travelling paths are shown in logarithmic scale.

Short and long-term remediation potential. In Figure 3, salinity is plotted against groundwater drawdown for 1974 until 2070; each arrow symbolizes one year. General behaviour shows increasing drawdown (due to pumping) and thus growing salinity. When pumping stops (2005), drawdown slowly recovers, but salinity continues rising at many locations, revealing a hysteresis: although there is no groundwater abstraction after 2005, hydraulic gradient still points from the sea into the pumps' direction. Hence, saline concentrations continue to increase. High salinization is possible even with only small drawdown (e.g. 'JT-69'), yet, maximum drawdown is up to 12 m within 30 years of pumping activity. Recovery times of groundwater levels are supposedly >100 a and even longer for salinity. Even when drawdown closes to zero (initial state), salinity is mostly higher than in the beginning of simulation (1974).

To assess long-term remediation capabilities, figure 4 shows heterogeneous patterns of Φ along the coast (see equation (1)). The isolines of Φ are relatively parallel to the coast line in the eastern area. Remediation potential appears to be relatively high as soon as abstraction is reduced. This may result from the aquifer's properties and high yield, and the corresponding preferred area of high abstraction activity. In the western area, the remediation potential is relatively high (due to a high mobility in porous media). The remediation potential drops where mobility is low. Low remediation potentials in the south of the coastal bay, where permeability is very low, might pose a reason for the development of the sabkha. Orange dots symbolize areas where the remediation potential does not fall below $0.5 \cdot c_{\text{rel}}$ within 500 years of simulation. Near-coastal dots are probably showing undisturbed situation of marine salinity intrusion (i.e. no groundwater abstraction). Dots further inland are due to low permeable hydrogeology. The PV pipeline processed the point-based Φ calculations as follows: data was filtered, to separate valid data from intentional output error values (e.g. $0.5 \cdot c_{\text{rel}}$ within 500 years); continuous data are generated from the point data by 2D Delaunay meshing over the area. Then, isolines of Φ were created.

4. Conclusions and Outlook

In the situation at hand, when model structures and simulation results are complex, proper visualization proofs to be an integral tool in the model development, data interpretation and decision making process. Utilization of various combinations of filters provide inside knowledge on proper model setup (e.g. heterogeneous structure and flow) and behaviour (e.g. areal distributed abstraction areas or density-induced convection near coast).

The visualized scenario simulation stresses the vulnerability of the local aquifer system, and the sensitive balance of the fresh-saltwater interface. The outcome underlines the necessity of an immediate action to prevent further saline intrusion or even total loss of the usability of the

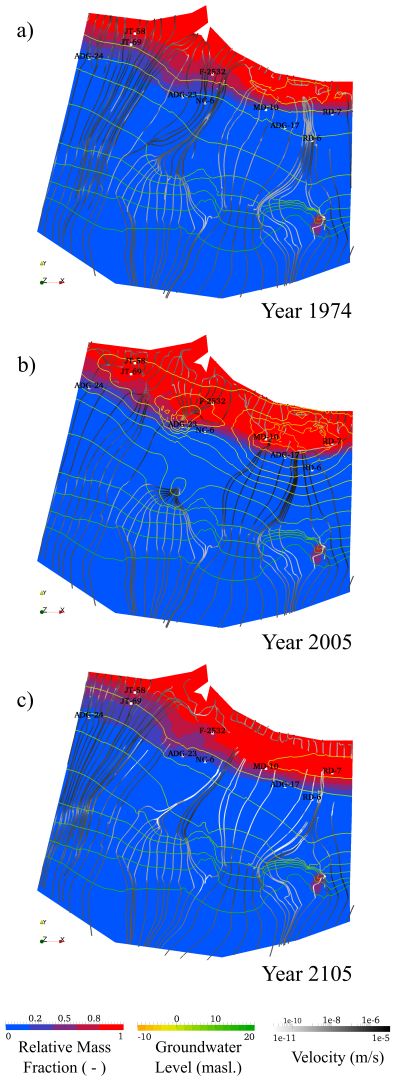

Figure 2: *Time series of salinity (at 10 m below groundwater level), groundwater levels (isolines), stream tracer, and selected observation wells.*

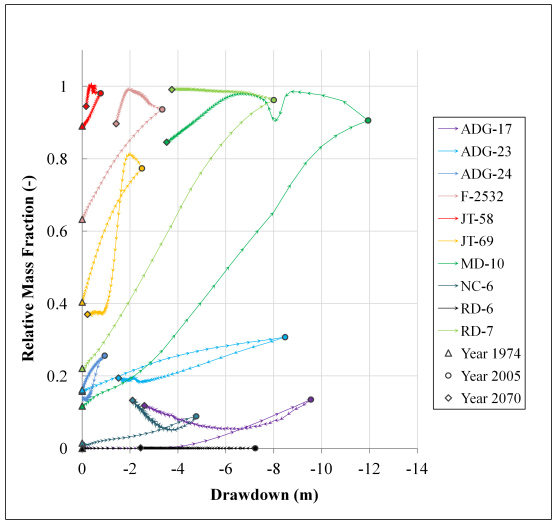

Figure 3: *Salinity vs. drawdown over time, simulation time 1974-2070, pumping activity stopped after 2005.*

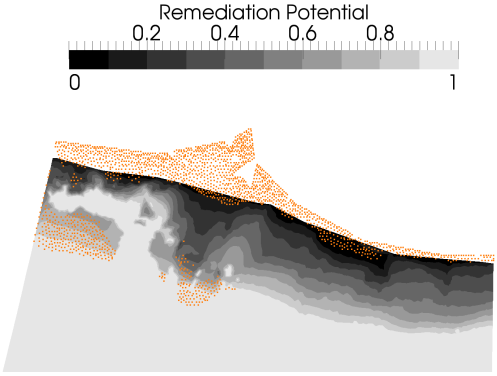

Figure 4: *Salinity remediation potential of coastal area 10 m below groundwater level (0 = low potential, 1 = high potential), based on salinity half-life after pump stop; orange dots do not reach half initial concentration within 500 years.*

local aquifer's groundwater resources. The interpretation of the simulation results would not have been successful without suitable visualization equipment and techniques. Model weaknesses were identified and the setup of the target area model (e.g. BC's, hydrogeology) and calibration (incl. comparison to real-world data) were substantially improved during the visualization and modelling procedure. Besides the presented 2D figures, the utilization of a virtual reality centre with a high-resolution video wall using stereoscopic projection and an optical tracking system gave inside knowledge on the model's behaviour and helped transporting scientific findings to Omani representatives supporting their decision making process.

5. Acknowledgments

The authors like to thank the anonymous reviewers for their valuable comments and acknowledge the funding by the German Federal Ministry of Education and Research (BMBF Number: FKZ 02WM1166), and by the Ministry of Science, Research and Arts of Baden-Württemberg (AZ Zu 33-721.3-2).

References

[BSKL12] BÖTTCHER N., SINGH A., KOLDITZ O., LIEDL R.: Non-isothermal, compressible gas flow for the simulation of an enhanced gas recovery application. *Journal of Computational and Applied Mathematics 236*, 18 (Dec. 2012), 4933–4943. doi:10.1016/j.cam.2011.11.013. 1

[Hen07] HENDERSON A.: *ParaView Guide, A Parallel Visualization Application*. Kitware Inc., 2007. URL: www.paraview.org. 2

[KBB*12] KOLDITZ O., BAUER S., BILKE L., BÖTTCHER N., DELFS J. O., FISCHER T., GÖRKE U. J., KALBACHER T., KOSAKOWSKI G., MCDERMOTT C. I., PARK C. H., RADU F., RINK K., SHAO H., SHAO H. B., SUN F., SUN Y. Y., SINGH A. K., TARON J., WALTHER M., WANG W., WATANABE N., WU Y., XIE M., XU W., ZEHNER B.: OpenGeoSys: an open-source initiative for numerical simulation of thermo-hydro-mechanical/chemical (THM/C) processes in porous media. *Environmental Earth Sciences 67*, 2 (Feb. 2012), 589–599. doi:10.1007/s12665-012-1546-x. 1

[KDS*11] KALBACHER T., DELFS J.-O., SHAO H., WANG W., WALTHER M., SAMANIEGO L., SCHNEIDER C., KUMAR R., MUSOLFF A., CENTLER F., SUN F., HILDEBRANDT A., LIEDL R., BORCHARDT D., KREBS P., KOLDITZ O.: The IWAS-ToolBox: Software coupling for an integrated water resources management. *Environmental Earth Sciences 65*, 5 (Aug. 2011), 1367–1380. doi:10.1007/s12665-011-1270-y. 1

[KGSW12] KOLDITZ O., GÖRKE U.-J., SHAO H., WANG W.: Thermo-Hydro-Mechanical-Chemical Processes in Porous Media: Benchmarks and Examples (Lecture Notes in Computational Science and Engineering). Springer, 2012. 1

[MAF12] MAF: *OMAN SALINITY STRATEGY (OSS) Oman Salinity Strategy*. Tech. rep., Ministry Of Agriculture And Fisheries (MAF), Sultanate Of Oman International Center For Biosaline Agriculture (ICBA) Dubai, UAE, 2012. 2

[NBK13] NAUMOV D., BILKE L., KOLDITZ O.: Rendering technique of multi-layered domain boundaries and its application to fluid flow in porous media visualizations. *this issue* (2013). 1

[PA08] PARK C.-H., ARAL M.: Saltwater intrusion hydrodynamics in a tidal aquifer. *Journal of Hydrologic Engineering 13*, September (2008), 863. 1

[SD87] SUGIO S., DESAI C. S.: Residual flow procedure for sea water intrusion in unconfined aquifers. *International Journal for Numerical Methods in Engineering 24*, 8 (Aug. 1987), 1439–1450. doi:10.1002/nme.1620240803. 1

[SML06] SCHROEDER W., MARTIN K., LORENSEN B.: *The Visualization Toolkit: An Object-oriented Approach to 3D Graphics*. Kitware, 2006. 2

[UKSD12] UNGER A., KLEMANN V., SCHULTE S., DRANSCH D.: A Visual Analytics Approach to Validate Geoscientific Simulation Ensembles. In *AGILE'2012 International Conference on Geographic Information Science* (Avignon, 2012), Gensel J., Josselin D., Vandenbroucke D., (Eds.), pp. 316–317. 1

[WDG*12] WALTHER M., DELFS J.-O., GRUNDMANN J., KOLDITZ O., LIEDL R.: Saltwater intrusion modeling: Verification and application to an agricultural coastal arid region in Oman. *Journal of Computational and Applied Mathematics 236*, 18 (Dec. 2012), 4798–4809. doi:10.1016/j.cam.2012.02.008. 1